Effects of atomic relaxation on phonon dispersion relations and thermal properties of ultrathin (Si)$_n$(Ge)$_n$[001] superlattices

Iorwerth O. Thomas and G. P. Srivastava

School of Physics, University of Exeter, Stocker Road, Exeter EX4 4QL, United Kingdom

Using *ab initio* density-functional perturbation theory we have examined the effects of atomic relaxation on the phonon dispersion relations and thermal properties of ultrathin (Si)$_n$(Ge)$_n$[001] ($1 \leqslant n \leqslant 5$) superlattices. It is found that atomic relaxation effects governed by the minimum energy requirement lead to significant changes in the location of phonon frequencies above 200 cm^{-1} as well as in the location and width of phononic gaps. These changes result in a decrease of around 7% in the zone-average phonon relaxation time and up to a 5% decrease in the thermal conductivity tensor components κ_{zz} and κ_{xx} of the (Si)$_1$(Ge)$_1$[001] superlattice.

I. INTRODUCTION

The nature of phonon transport in nanostructures is likely to play an important role in the development of improved semiconductor technologies. One example is the enhancement of the thermoelectric figure of merit through phonon confinement, and the reduction in phonon lifetime due to interface scattering and modified anharmonic interactions in nanostructured composite structures such as thin superlattices, nanowires, and nanodots.[1,2] The basic features of phonon transport in a system originate in its lattice dynamics, viz. phonon dispersion relations. The implementation of the equilibrium lattice constant, equilibrium bond lengths, and appropriate bond strengths is important for the accuracy of lattice dynamical calculations in composite nanostructure systems. Although the consideration of a weighted lattice constant for a composite of two compounds X and Y is a reasonable assumption, it is well known that the interatomic X-X, Y-Y, and X-Y bond lengths and corresponding bond strengths are inconsistent with the prediction of the weighted average scheme. The proper treatment of such effects is extremely important, especially for thin composite nanotructures made from materials of dissimilar atomic radii and dissimilar bond strengths.

In the 1980s and 1990s, several phenomenological and first-principles lattice dynamical calculations were carried out for ultrathin semiconductor superlattices,[3–15] but none employed fully relaxed cell size and atomic geometry. The theories adopted in those studies were either not capable of determining the equilibrium lattice constant, individual bond lengths, and hetero bond strengths through geometric relaxation, or did not examine it, with the exception of Wei *et al.*'s calculation of the shear modulus in bulk Si and Ge and in superlattices.[11] As a result, there are no accurate reports of the effects of atomic relaxations in phonon spectrum and related properties for thin superlattices made of lattice-mismatched materials, such as Si/Ge. Recently, we have studied the lattice dynamics using an adiabatic bond charge model, paying particular attention to one-dimensional phononic gaps in thin semiconductor superlattices.[16–18] More recently, Garg *et al.* have examined the thermal conductivity of ultrathin superlattices using the virtual crystal approximation (in general) and a full calculation for the thinnest case.[19]

In this study, we perform an *ab initio* investigation of the effects of atomic relaxation on phonon dispersion curves, density of states, the tensor η representing the zone-average product of the specific heat and square of phonon velocity, zone-average anharmonic phonon relaxation time $\langle \tau \rangle$, and the phonon conductivity tensor κ for ultrathin (Si)$_n$(Ge)$_n$ superlattices ($1 \leqslant n \leqslant 5$), where n denotes the number of Si and Ge bilayers within the period of repetition along the superlattice growth direction. In many ways this is an idealized system, but this idealization is necessary in order that we be able to distinguish this effect from other, perhaps more significant ones.

II. THEORETICAL AND COMPUTATIONAL DETAILS

In order to determine the equilibrium lattice constant, interatomic bond lengths, and phonon dispersion relations, we made use of the density functional peturbation theory (DFPT) package included in QUANTUM ESPRESSO,[20] utilizing the plane wave pseudopotential method and the local density approximation (LDA) of the density functional theory. All calculations for the superlattices (Si)$_n$(Ge)$_n$[001] with $n =$ 1-5- were performed at $a_0 = 5.54$ Å, the Vegard average of the experimental lattice constants of Si and Ge. For brevity we will refer to a superlattice (Si)$_n$(Ge)$_n$[001] as SL(n,n). Computational details involve the use of norm-conserving pseudopotentials from Ref. 21, a plane-wave basis set up to the kinetic energy cutoff of 15 Ry, and Brillouin zone integrations for the electronic (phonon) calculations by by using $10 \times 10 \times 2$ shifted (unshifted) Monkhorst-Pack (MP) grids.[22] We performed phonon calculations for three cases: no atomic relaxation, atomic relaxation in the growth (z) direction only (for $n = 1$–4), and full atomic relaxation in all directions ($z = [001]$, $x = [110]$, and $y = [1\bar{1}0]$). "Bulk" values for Si (Ge) were generated by exchanging Ge (Si) atoms with (Si) Ge atoms in (2,2) SL cells, and using a lattice constant of 5.42 (5.66) Å, close to the LDA value. We observe that our choice of the cubic lattice constant a_0 is only 1.5% larger than Wei *et al.*'s[11] LDA equilibrium result and should not lead to any significant changes to the conclusions reached from this study.

The anharmonic phonon relaxation time was numerically evaluated by using the following expression which includes

contributions from optical modes based on an extension of previous treatments,[23,24] as discussed in Ref. [25]:

$$\tau_{\mathrm{AH}}^{-1}(\boldsymbol{q}s)$$

$$= \frac{\pi \hbar \bar{\gamma}^2}{\rho V} \sum_{\boldsymbol{q}'s',\boldsymbol{q}''s'',\boldsymbol{G}} \frac{(\mathcal{B}_{\boldsymbol{q}s,\boldsymbol{q}'s',\boldsymbol{q}''s''})^2}{\omega(\boldsymbol{q}s)\omega(\boldsymbol{q}'s')\omega(\boldsymbol{q}''s'')} \mathrm{DM}(\boldsymbol{q}s,\boldsymbol{q}'s',\boldsymbol{q}''s'')$$

$$\times \left[\frac{\bar{n}_{\boldsymbol{q}'s'}(\bar{n}_{\boldsymbol{q}''s''}+1)}{(\bar{n}_{\boldsymbol{q}s}+1)} \delta(\omega(\boldsymbol{q}s)+\omega(\boldsymbol{q}'s')\right.$$

$$-\omega(\boldsymbol{q}''s''))\delta_{\boldsymbol{q}+\boldsymbol{q}',\boldsymbol{q}''+\boldsymbol{G}} + \frac{1}{2}\frac{\bar{n}_{\boldsymbol{q}'s'}\bar{n}_{\boldsymbol{q}''s''}}{\bar{n}_{\boldsymbol{q}s}}\delta(\omega(\boldsymbol{q}s)$$

$$\left. -\omega(\boldsymbol{q}'s')-\omega(\boldsymbol{q}''s''))\delta_{\boldsymbol{q}+\boldsymbol{G},\boldsymbol{q}'+\boldsymbol{q}''} \right], \tag{1}$$

where $\boldsymbol{q}$ is the phonon wave vector, s labels a phonon branch, the magnitude of the velocity for a given mode $\boldsymbol{q}s$ is $c_s(\boldsymbol{q})$, the frequency of that mode is $\omega(\boldsymbol{q}s)$, $\bar{n}_{\boldsymbol{q}s}$ gives the equilibrium Bose-Einstein distribution, and

$$\mathcal{B}_{i,j,k} = [\sqrt{\omega(i)\omega(j)}[\omega(i)+\omega(j)]|\omega_\Gamma(k)-\omega(k)|/c(k)$$

$$+ \text{ similar terms with } i, j, \text{ and } k \text{ interchanged}]/3!, \tag{2}$$

where $\omega_\Gamma(k)$ is the Γ point (zone center) frequency for mode k, with $c(k)$ being the phonon speed for the branch and momentum labeled by k. Normal (Umklapp) processes are accounted for by zero (nonzero) reciprocal lattice vectors $\boldsymbol{G}$, and the strength of the the anharmonic phonon interaction is controlled by $\bar{\gamma}$, which is the mode-averaged rescaled Grünneissen constant. The term $\mathrm{DM}(\boldsymbol{q}s,\boldsymbol{q}'s',\boldsymbol{q}''s'')$ in Eq. (1) is the *dual mass term* arising from the presence of two materials in the superlattice:[26]

$$\mathrm{DM}(\boldsymbol{q},\boldsymbol{q}',\boldsymbol{q}'') = \frac{1}{64}\left(\frac{\mathcal{A}_{AB}}{2\rho_A^{3/2}} + \frac{\mathcal{A}_{BA}}{2\rho_B^{3/2}}\right)^2 \tag{3}$$

where

$$\mathcal{A}_{ij} = 1 + \frac{\rho_i^{1/2}}{\rho_j^{1/2}}\left(\frac{e_j}{e_i} + \frac{e_j'}{e_i'} + \frac{e_j''}{e_i''}\right)$$

$$+ \frac{\rho_i}{\rho_j}\left(\frac{e_j e_j'}{e_i e_i'} + \frac{e_j' e_j''}{e_i' e_i''} + \frac{e_j e_j''}{e_i e_i''}\right) + \frac{\rho_i^{3/2}}{\rho_j^{3/2}}\left(\frac{e_j e_j' e_j''}{e_i e_i' e_i''}\right), \tag{4}$$

$\rho_{A(B)}$ is the density of material A (B) and the amplitudes of the eigenvectors $e_{A(B)}$ are given by the the solution to the one-dimensional linear-chain model (as per Ref. [18]):

$$\frac{e_B}{e_A} = \frac{\left[\frac{1}{M_0} - \Delta\left(\frac{1}{M}\right)\right]\cos(l_z q_z)}{\left[\left(\frac{1}{M_0}\right)^2 + \left\{\Delta\left(\frac{1}{M}\right)\right\}^2 \sin^2(l_z q_z)\right]^{1/2} - \Delta\left(\frac{1}{M}\right)}. \tag{5}$$

In the above, $M_0 = (M_A^{-1} + M_B^{-1})/2$, $\Delta(1/M) = (M_A^{-1} - M_B^{-1})/2$, and l_z is the length of the superlattice period in the z direction.

The lattice thermal conductivity tensor was computed within the single-mode approximation, using the expression[27]

$$\kappa_{\mu\nu} = \frac{\hbar^2}{3Vk_\mathrm{B}T^2} \sum_{\boldsymbol{q}s} c_\mu(\boldsymbol{q}s)c_\nu(\boldsymbol{q}s)\omega^2(\boldsymbol{q}s)\tau(\boldsymbol{q}s)\bar{n}_{\boldsymbol{q}s}(\bar{n}_{\boldsymbol{q}s}+1), \tag{6}$$

where $c_\mu(\boldsymbol{q}s)$ is the μth component of the group velocity for phonon mode $\boldsymbol{q}s$ and $V = N_\mathrm{cell}\Omega_0$ is the total volume of the system; Ω_0 is the volume of a unit cell and N_cell is the number of unit cells present.

III. RESULTS

A. Atomic geometry and phonon dispersion curves

Figure 1 shows the Si and Ge atomic layers along the (1,1) SL growth direction (left panel), and the bond relaxation results for the (n,n) SL for $n = 1$–3 (right panel) (results for $n = 4, 5$ are qualitatively similar to those displayed). Typically, as expected in (n,n) SLs the Si-Ge bond length (2.40 Å) is almost the same as $(\sqrt{3}/4)a_0$, but compared to this value a Si-Si bond length shrinks by around 0.02–0.03 Å and a Ge-Ge bond length expands by 0.02–0.03 Å. Thus the Si (Ge) layer contracts (expands) by approximately 0.8% to 1% compared to the bulk average value. Allowing relaxation in all directions and allowing it in only the z direction for $n = 1$–4 gives rise to no significant differences; this suggests that the majority of the strain exerted on the system is in the z direction. We should note that our quoted relaxed results are for relaxation in all directions.

We first note that the formation of the Si/Ge SL structure gives rise to generation of band gaps for longitudinal as well as transverse phonon branches. Interatomic bond length relaxation is found to produce changes in phonon dispersion relations of the (n,n) SL in general, as well as properties directly related to these. Changes in the dispersion curves can be most clearly illustrated for the (1,1) SL (Fig. 2). We now note a few details of the lower (below 200 cm^{-1}) and upper (above 400 cm^{-1}) regions of the spectrum. For the unrelaxed geometry, the second and third transverse branchs are found to be split at the zone edge X along the SL growth direction. These branches become degenerate, with frequency $\approx$90 cm^{-1}, when the relaxed geometry is used. The central frequency and splitting between the third and fourth transverse branches at the zone center (Γ) are, respectively, $\approx$112 (113) cm^{-1} and $\approx$15 (13) cm^{-1} for the unrelaxed (relaxed) geometries. The central frequency and splitting between the first and second longitudinal branches at the zone edge X are, respectively, $\approx$173 (171) cm^{-1} and $\approx$54 (48) cm^{-1} for the unrelaxed (relaxed) geometries. The effect of relaxation is to increase the splitting between the tenth and eleventh (out of twelve) branches which lie around 400 cm^{-1}: at the zone center this splitting increases by $\approx$9 cm^{-1}. The most dramatic changes resulting from atomic relaxation are the location and dispersion of the two highest (viz. eleventh and twelfth) branches. The eleventh branch is almost dispersionless for both relaxed and unrelaxed geometries, but is shifted upwards by $\approx$6 cm^{-1} when the relaxed geometry is used. The effect of the relaxed geometry is to produce only a little change to the dispersion but
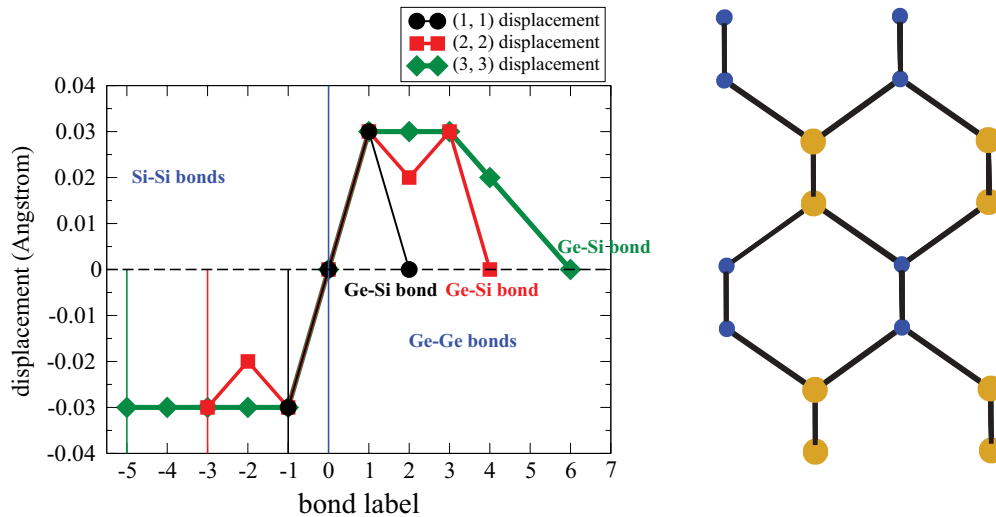
FIG. 1. (Color online) Bond relaxation in $(Si)_n(Ge)_n$[001] superlattices with n ranging from 1 to 3 (left). The zeroth bond is the Si-Ge bond at the center of the z axis of the cell; the vertical lines in the Si-Si half of the plot indicate the boundary of the cell, and the Ge-Si bonds that terminate the cell in the Ge-Ge half of the plot are labeled approprately. Atomic positions for the (1,1) superlattice (right) are shown in order to clarify the arrangement of the atomic bonds.

a huge upward shift by $\approx$28 cm^{-1} (0.84 THz) in the frequency location of the highest (twelfth) branch.

Examining the phonon density of states (PHDOS) plots in Fig. 3 for all the SL studied, we find that relaxation introduces significant modifications at high frequencies, consistent with the dispersion curves. In all cases, it shifts the maximum frequency observed in the system upwards, and for $n > 1$ shifts the location of the most prominent peaks while maintaining their general qualitative structure. At $n = 1$ this is not the case for frequencies above 400 cm^{-1}, where relaxation causes a distinct change in the shape of the PHDOS curve. The low-frequency regions of the PHDOS in all cases seem to be relatively unchanged following relaxation, suggesting that it is the properties of the high-lying optical modes which are most affected by relaxation. We note that there exists a distinct gap in the PHDOS for $n = 1$, corresponding to a three-dimensional phononic gap.

It is interesting and instructive to examine the variations of the zone-center optical mode frequencies with the SL thickness. Following Refs. 28 and 29, we have fitted the

variation of the highest mode as

$$\omega_{\text{highest}}^2(n) = \omega_\infty^2 - \frac{A}{n^2},\qquad(7)$$

where A is a constant and ω_∞ represents the highest frequency for the limiting case $n \to \infty$ (essentially being close to the average of zone-center optical values for bulk Si and Ge). We obtained $\omega_\infty = 480$ cm^{-1} and $A = 47\,257$ cm^{-2} in the unrelaxed case, and $\omega_\infty = 493$ cm^{-1} and $A = 50\,718$ cm^{-2} in the relaxed case. Following an earlier work[28] we attempted an *ad hoc* fit of the form $\omega_{\text{lowest}}^2 = B/n^\alpha$, with $B = 106$ cm^{-1} and $\alpha = 0.47$ in the relaxed case and $B = 105$ cm^{-1} and $\alpha = 0.46$ in the unrelaxed case. However, it seems that the following expression also provides a good fit to our numerical data:

$$\omega_{\text{lowest}}^2(n) = \omega_{\text{lowest}}^2(1)\left[\frac{\text{Si}(\pi/2n)}{\text{Si}(\pi/2)}\right]^{1/2},\qquad(8)$$
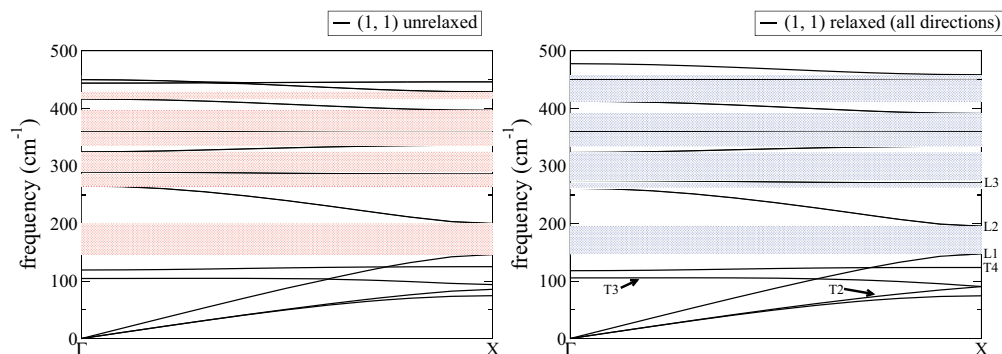

FIG. 2. (Color online) Phonon dispersion in the z direction for the Si/Ge(1,1)[001] superlattice. Shaded regions indicate phononic gaps.
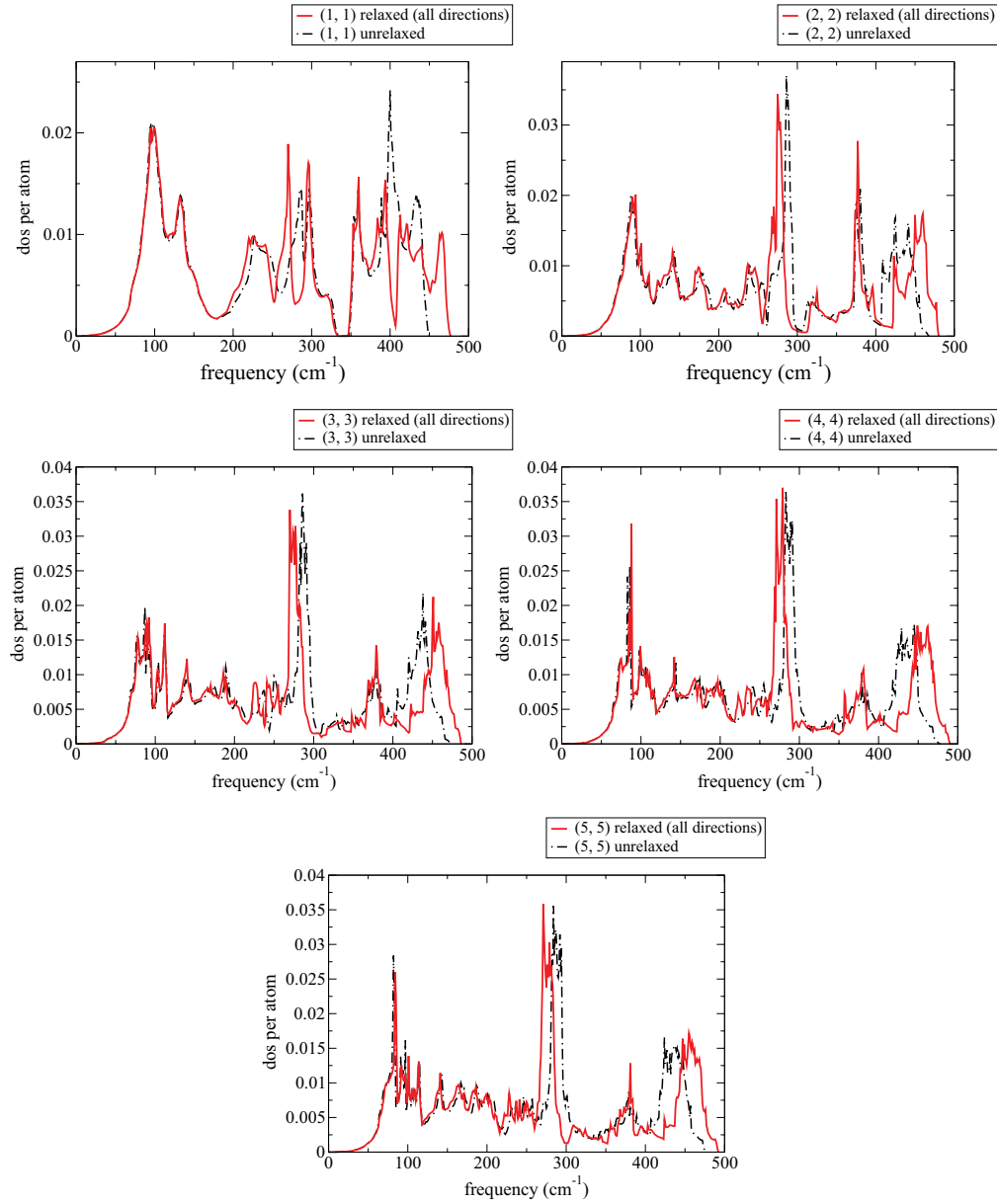
FIG. 3. (Color online) Phonon density of states for $(\text{Si})_n(\text{Ge})_n[001]$ superlattices. Solid lines represent fully relaxed cases, dashed lines relaxation in the z direction only, and dot-and-dashed lines represent the unrelaxed case.

where $\text{Si}(x) = \int_0^x \frac{\sin t}{t} dt$ is the sine integral function.[30] We display a plot of fits (7) and (8) alongside the data in Fig. 4.

B. Effect of atomic relaxation on thermal properties

The effect of atomic relaxation may lead to changes in thermal properties in two ways. The first is through changes in phonon velocities and frequencies, and the second is through phonon scattering rates. It should be noted that the changes in the latter category are heavily influenced by the changes in the former category. In brief, phonon-defect and phonon-phonon scattering rates increase with some power(s) of phonon frequency. Thus the calculated atomic-relaxation related upward shifts in optical phonon frequencies will significantly alter phonon lifetimes. In particular acoustic-optical phonon scattering rates, being highly dependent on

optical phonon frequencies, may significantly affect the lattice thermal conductivity.[31–33] We will examine three quantities to study the effect of atomic relaxation.

1. Tensor $\{\eta_{\mu\nu}\}$

First, we examine the tensor $\{\eta_{\mu\nu}\}$ formed by the mode average of the product of specific heat and square of phonon velocity:[14,15]

$$\eta_{\mu\nu} = \sum_{qs} \frac{\kappa_{\mu\nu}(qs)}{\tau(qs)} = \sum_{qs} C_v(qs)c_\mu(qs)c_\nu(qs), \quad (9)$$

where $\mu, \nu = x, y, z$, and C_v is the specific heat. Hyldgaard and Mahan[14] and Tamura *et al.*[15] have previously examined the behavior of η_{zz} in SLs, but did not examine the planar behavior and could not treat the effects of bond relaxation as
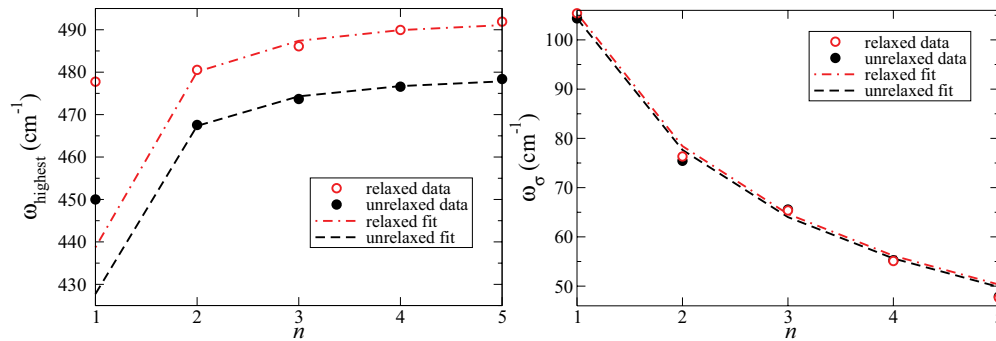
FIG. 4. (Color online) Variation of the highest zone center frequency ω_{highest} and the lowest nonzero zone center frequency (ω_σ) with the SL size index n.

they employed phenomenological lattice dynamical models which cannot describe geometric relaxation. The phonon eigensolutions required for this calculation were generated from the force constants generated on a $10 \times 10 \times 2$ MP grid in the aforementioned DFPT calculations; they were computed on more fine-grained grids in order to attain good convergence of $\eta_{\mu\nu}$ (convergence was tested for the $n = 1$ system at $T = 10, 20, 100$, and 1200 K). The grids used are $16 \times 16 \times 12$ ($n = 1$), $16 \times 16 \times 6$ ($n = 2$), and $16 \times 16 \times 4$ ($n = 3, 4, 5$). As discussed above, bulk values were calculated using (2,2)-type cells where all atoms were of the required species.

Figure 5 shows the results for the specific heat C_v and η_{zz}. The specific heat is similar for SLs of any layer thickness index n, with values lower than the average of the bulk value and becoming almost constant for $T > 600$ K; we do not display the unrelaxed results for they are more or less identical to the relaxed results. The quantity η_{zz}, on the other hand, is in general lower than the value for either of bulk Si or Ge, becomes almost constant when $T > 300$ K, and generally decreases as n increases. This is consistent with the findings of Ref. 15 in which it is found that as n increases, η_{zz} successively converges on values which are much smaller than those for bulk Ge.

As the main difference between C_v and η arises from the inclusion of the phonon velocity in the definition of the latter, we conclude that the trend in η_{zz} with SL layer thickness is governed by the alteration of the phonon velocity component along the growth direction as n is increased, as previously determined in Refs. 14 and 15. In Fig. 6 we plot the ratios

of values of $\eta_{\mu\nu}$ in various directions at $T = 1200$ K as n is varied. We find that η_{xx} and η_{yy} are larger than η_{zz} for all n. This should not be surprising, since the Si-Ge interface should act to suppress phonon transport in the z direction. η_{xx} is smaller than η_{yy} for $n = 1$, indicating a degree of planar anisotropy in the system. However, once n is increased above unity their values become similar and the anisotropy all but vanishes. This appears to be because the bilayers on either side of at least one of the Si-Ge interfaces are anisotropically arranged with respect to these directions when n is odd; for odd $n > 1$ this effect would be subordinate to dominant effects arising from the presence of isotropically arranged bilayers within the Si and Ge multilayers. However, the $n = 1$ superlattice is *nothing but* a sequence of bilayers on either side of the Si-Ge interface, and so the anisotropy is particularly apparent. For systems with even n, the multilayers are always arranged in an isotropic fashion, hence the ratio η_{yy}/η_{xx} is much closer to 1 than in the cases when it is odd.

The general behavioral trend of η in the planar directions as n is increased is not generally the same as it is in the z direction; in fact it is difficult to identify a precise pattern. However, at $T = 1200$ K, η_{xx} for the SLs are within a distance of around 9% from the bulk Ge value of $\eta_{xx} = 0.01592$ W K^{-1}cm^{-1}ps^{-1} for all n, and for η_{yy} the values are within around a distance of around 12% from the bulk value for $n > 1$ (which is identical to the bulk η_{xx} value). For $n = 1$, η_{yy} is slightly smaller than the *average* of the two bulk values. Similar qualitative observations can be made for the planar components of η at other high temperatures.
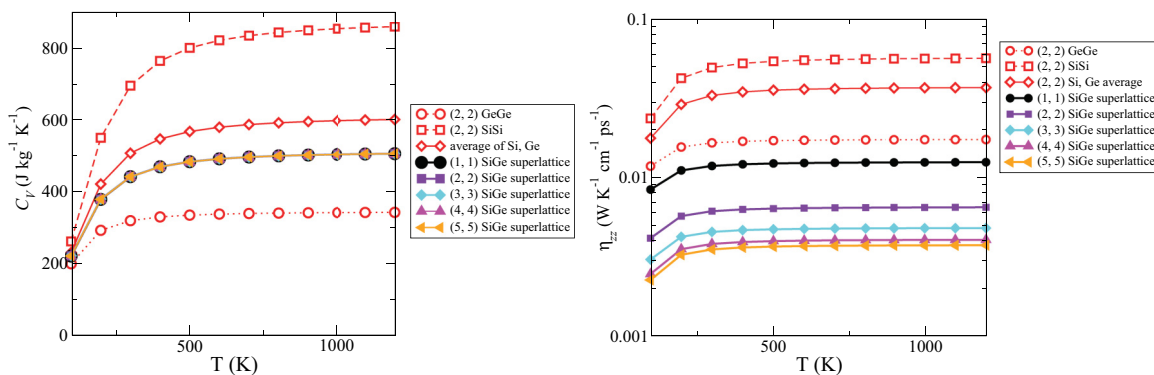

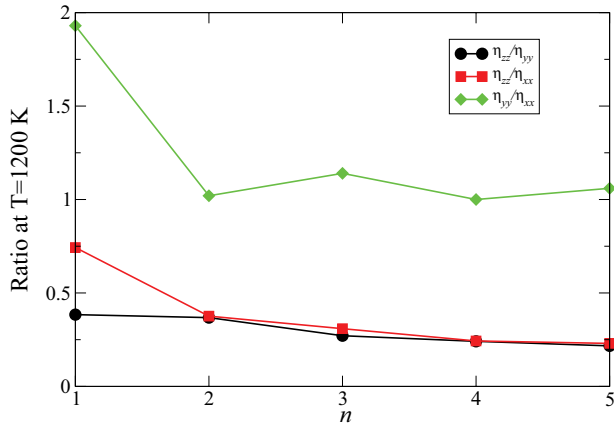FIG. 5. (Color online) Plot of C_v and η_{zz} for various systems.

FIG. 6. (Color online) Plot of the ratios of $\eta_{\mu\nu}$ values in the x, y, and z directions.

For η_{zz} (Fig. 7) we find that relaxation of the geometry makes little difference in the (1,1) case (around 1.6% of the smaller value at $T = 1200$ K), slightly more difference in the (2,2) case (around 3.9% of the smaller value at $T = 1200$ K)—where the unrelaxed results are smaller than the relaxed results—and for $n \geqslant 3$ (where the unrelaxed results are larger than the relaxed results), the shifts due to relaxation are fairly similar to each other: for $n = 3, 4, 5$ we have shifts of around 4.8%, 5.96%, and 6.98% of the smaller values at $T = 1200$ K respectively. In the case of the planar directions,

we find that the effects of relaxation are more limited: the largest shifts at $T = 1200$ K are at $n = 1$ for η_{yy} (around 2.2% of the smallest value) and $n = 3$ and 4 for η_{xx} (both around 1.2% of the smallest value). That η_{zz} is the most affected by relaxation would be consistent with what we've seen of the effects of bond relaxation, which only have a significant effect on the location of atoms in the growth direction. We note that while our results are in qualitative agreement with the studies carried out by Hyldgaard and Mahan[14] and Tamura *et al.*,[15] the present *ab initio* calculations including full atomic relaxation provide numerically more accurate results.

2. Phonon relaxation time

The anharmonic phonon relaxation time for SL(1,1) was computed using Eq. (1), with a rescaled average Grüneisen constant of 0.5, and considering all allowed normal and Umklapp three-phonon processes. A set of 14 superlattice reciprocal lattice vectors $\boldsymbol{G}$ were included for evaluating Umklapp scattering rates. The *dual mass term* $DM(\boldsymbol{q}s, \boldsymbol{q}'s', \boldsymbol{q}''s'')$ was included following the prescription adopted in our group's previous work;[18] the Kronecker delta symbol constraining the value of q'' and the energy Dirac delta function were handled as described in Ref. 25 (with $\sigma = 0.0081$ in the latter case) and the summation over q' was carried out using the $16 \times 16 \times 12$ MP grid.

The zone-average results for the phonon anharmonic relaxation time are shown in Fig. 8; they clearly indicate that
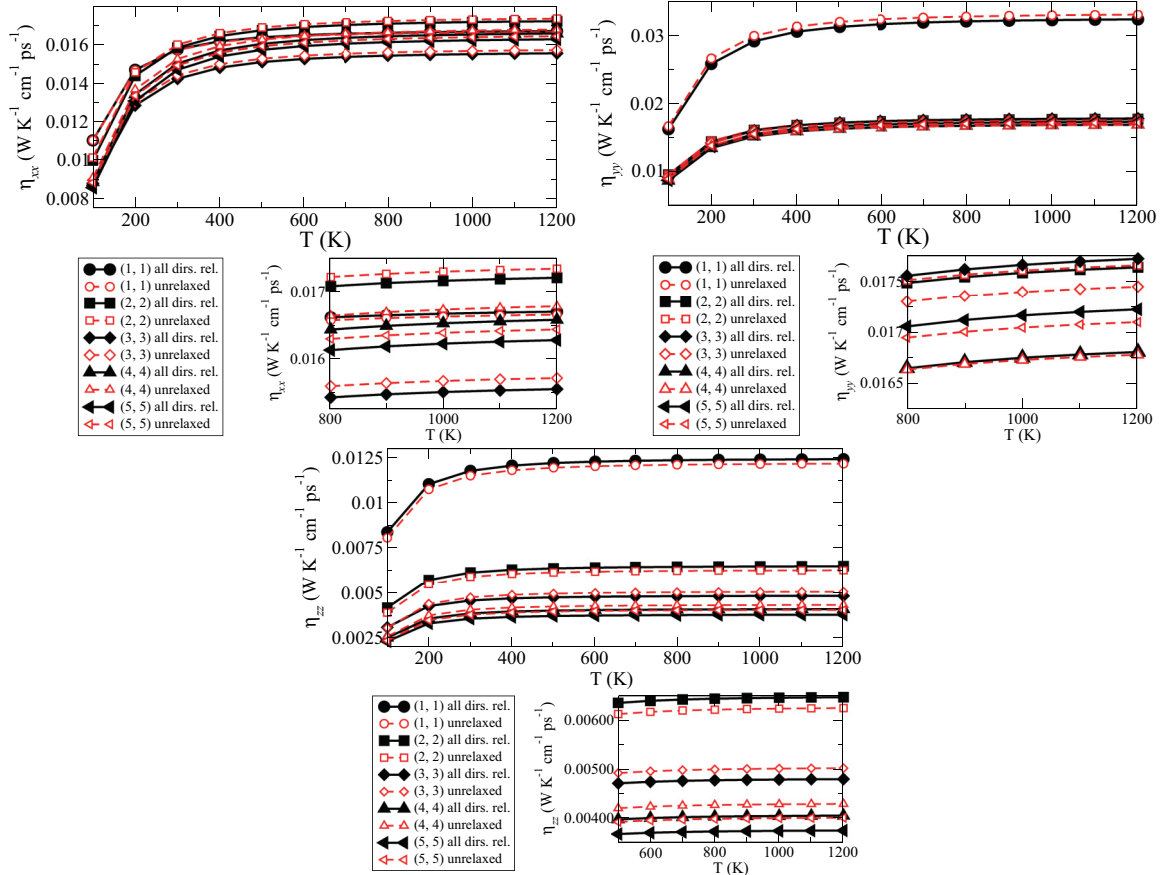

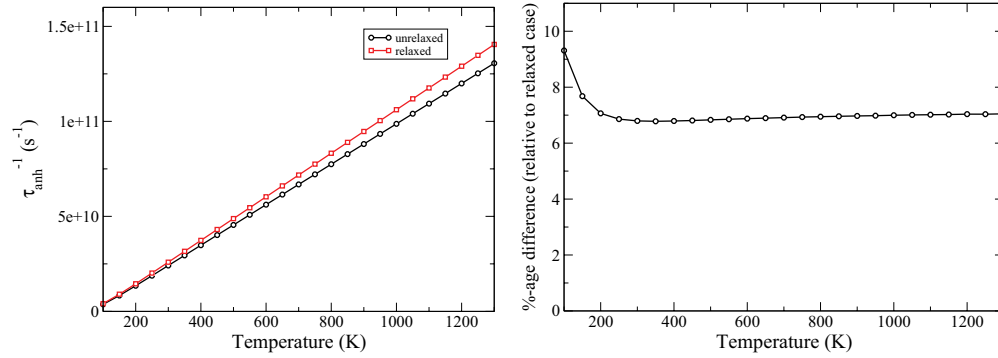FIG. 7. (Color online) Comparison of $\eta_{\mu\nu}$ for various systems.

FIG. 8. (Color online) Zone-average anharmonic phonon relaxation time for Si/Ge(1,1)[001]. The right-hand panel shows the percentage increase in the relaxation rate arising from the atomic relaxation required for the total energy of the system to be at its minimum.

atomic relaxation noticeably alters the relaxation rate at high temperatures. The right-hand panel of this figure shows the percentage increase in the anharmonic scattering time caused by the inclusion of relaxation in the calculation. While there are no studies available with which we can compare our results, we can conclude from this that atomic relaxation can increase the anharmonic phonon relaxation rate by around 7% as we approach and surpass room temperature.

3. Thermal conductivity tensor $\{\kappa_{\mu\nu}\}$

The lattice thermal conductivity was evaluated for SL(1,1). The total phonon relaxation rate for each phonon mode over the $16 \times 16 \times 12$ MP grid was obtained via Matthiessen's rule through adding contributions from boundary scattering, mass defect scattering (which for the $n = 1$ case includes both alloy and isotope scattering), and three-phonon anharmonic interactions as described in Ref. 25. As in that previous study,[25] we used an effective boundary length of 0.2 μm, but other parameters were set differently: the mass defect parameter P was taken to be to be 1.0 and $\bar{\gamma}$ to be 0.5. The conductivity results, with unrelaxed and relaxed atomic geometries, are shown in Fig. 9. The in-plane component κ_{xx} of the conductivity is bigger than the component κ_{zz} along the SL growth direction for all temperatures, which is consistent with the behavior of the tensor η. For SL(1,1) the ratio κ_{xx}/κ_{zz} is found to be close to 1.2 at $T = 1200$ K.

The right-hand panel in Fig. 9 shows the percentage decrease in κ_{xx} and κ_{zz} when atomic relaxation is included in the computation. The difference is appreciable for temperatures larger than 300 K. For example, κ_{zz} decreases by almost 4% and κ_{xx} decreases by slightly more than 5% once we pass $T = 1200$ K, changes that are more significant than those observed in η for this SL. From our numerical calculations we establish that the effect of atomic relaxation on the $\kappa_{\mu\nu}$ components cannot simply be obtained as the product of the effects for $\eta_{\mu\nu}$ and $\tau_a v$. This can be understood if one observes that the effect of atomic relaxation on each of these quantities may be different for different q points in the Brillouin zone.

IV. SUMMARY

In summary, we have shown that an *ab initio* account of crystal geometry (lattice constant and bond lengths) obtained from the minimization of total energy and interatomic forces demonstrates important changes in predictions of the energy spectrum of phonons above 200 cm^{-1} in ultrathin $(Si)_n(Ge)_n$ superlattices. These in turn result in alterations to the predicted results for phononic properties (locations of phononic gaps and their widths) and thermal properties. Numerical calculations suggest that the product of the specific heat and phonon velocity squared, η, is more affected by the geometry relaxation along the SL growth direction than in a SL plane direction.
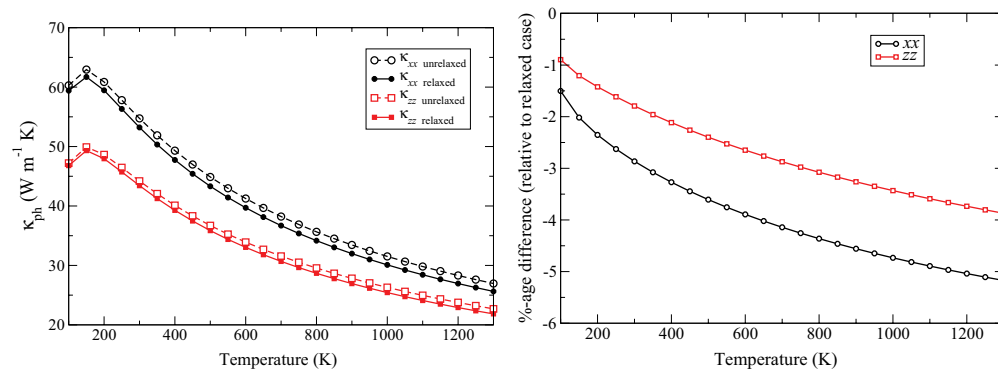

FIG. 9. (Color online) Lattice thermal conductivity of Si/Ge(1,1)[001] using unrelaxed as well as relaxed atomic geometries. The right-hand panel shows the percentage decrease in the results arising from the atomic relaxation.

The zone-average value of the phonon anharmonic relaxation time in the $(Si)_1(Ge)_1$ superlattice is increased by around 7%. Finally, the overall effect of atomic relaxation is to reduce the values of the phonon conductivity tensor components by approximately 3%–5%. We should observe, however, that these changes may be swamped in more realistic, less ideal systems by the magnitude of other effects, for instance surface roughness.

Our findings for ultrathin Si/Ge superlattices highlight the effects of fully relaxing the geometry of a structure in first-principles studies of phonon spectrum, phonon interac-

tions, and thermal properties of nanostructured composite systems.

[1] G. Chen, M. S. Dresselhaus, G. Dresselhaus, J.-P. Fleurial, and T. Caillat, Int. Mater. Rev. **48**, 45 (2003).

[2] J.-C. Zheng, Front. Phys. China **3**, 269 (2008).

[3] A. Fasolino and E. Molinari, J. Phys (Paris), Colloq. C **5**, 569 (1987); E. Molinari and A. Fasolino, Appl. Phys. Lett. **54**, 1220 (1989).

[4] S.-F. Ren, H. Chu, and Y.-C. Chang, Phys. Rev. B **37**, 8899 (1988).

[5] M. I. Alonso, F. Cordeira, D. Niles, and M. Cardona, J. App. Phys. **68**, 5645 (1989).

[6] J. Zi, K. Zhang, and X. Xie, Chin. Phys. Lett. **6**, 230 (1990); J. Phys.: Condens. Matter **2**, 2473 (1990); Phys. Rev. B **41**, 12862 (1990).

[7] S. Baroni, P. Giannozzi, and E. Molinari, Phys. Rev. B **41**, 3870 (1990).

[8] R. A. Ghanbari, J. D. White, G. Fasol, C. J. Gibbings, and C. G. Tuppen, Phys. Rev. B **42**, 7033 (1990).

[9] E. Molinari, S. Baroni, P. Giannozzi, and S. de Gironcoli, Phys. Rev. B **45**, 4280 (1992).

[10] S. de Gironcoli, Phys. Rev. B **46**, 2412 (1992).

[11] S. Wei, D. C. Allan, and J. W. Wilkins, Phys. Rev. B **46**, 12411 (1992).

[12] S. de Gironcoli, E. Molinari, R. Schorer, and G. Abstreiter, Phys. Rev. B **48**, 8959 (1993); R. Schorer, G. Abstreiter, S. de Gironcoli, E. Molinari, H. Kibbel, and H. Presting, *ibid.* **49**, 5406 (1994).

[13] Z. V. Popović, E. Richter, J. Spitzer, M. Cardona, A. J. Shields, R. Nötzel, and K. Ploog, Phys. Rev. B **49**, 7577 (1994).

[14] P. Hyldgaard and G. D. Mahan, Phys. Rev. B **56**, 10754 (1997).

[15] S. I. Tamura, Y. Tanaka, and H. J. Maris, Phys. Rev. B **60**, 2627 (1999).

[16] S. P. Hepplestone and G. P. Srivastava, Phys. Rev. Lett. **101**, 105502 (2008).

[17] S. P. Hepplestone and G. P. Srivastava, J. Appl. Phys. **107**, 043504 (2010).

[18] S. P. Hepplestone and G. P. Srivastava, Phys. Rev. B **84**, 115326 (2011).

[19] J. Garg, N. Bonini, and N. Marzari, Nanoletters **11**, 5135 (2011).

[20] P. Gianozzi *et al.*, J. Phys.: Condens. Matter **21**, 395502 (2009); code available from http://www.quantum-espresso.org.

[21] We used the pseudopotentials Si.pz-vbc.UPF and Ge.pz-bhs.UPF, which are available from http://www.quantum-espresso.org.

[22] H. J. Monkhorst and J. D. Pack, Phys. Rev. B **13**, 5188 (1976).

[23] P. G. Klemens, in *Solid State Physics*, edited by F. Seitz and D. Turnbull, Vol. 7 (Academic, New York, 1958) p. 1; Phys. Rev. **122**, 443 (1961); **148**, 845 (1966).

[24] B. K. Ridley and R. Gupta, Phys. Rev. B **43**, 4939 (1991).

[25] I. O. Thomas and G. P. Srivastava, Phys. Rev. B **86**, 045205 (2012).

[26] S. Y. Ren and J. D. Dow, Phys. Rev. B **25**, 3750 (1982).

[27] G. P. Srivastava, *The Physics of Phonons* (Adam Hilger/IOP, Bristol, 1990).

[28] S. P. Hepplestone and G. P. Srivastava, Nanotechnology **17**, 3288 (2006).

[29] B. Jusserand, D. Paquet, F. Mollot, F. Alexandre, and G. Le Roux, Phys. Rev. B **35**, 2808 (1987).

[30] M. Abramowitz and I. A. Stegun, *Handbook of Mathematical Functions* (Eighth Printing), (Dover, New York, 1972).

[31] G. P. Srivastava, in *Proceedings of the Third International Conference on Phonon Scattering in Condensed Matter, Brown University, 1979*, edited by Humphrey J. Maris (Plenum, New York, 1980), p. 149.

[32] G. P. Srivastava, J. Phys. Chem. Solids **41**, 357 (1980).

[33] Z. Tian, J. Garg, K. Esfarjani, T. Shiga, J. Shiomi, and G. Chen, Phys. Rev. B **85**, 184303 (2012).